ARTICLE

doi:10.1038/nature12149

Pif1 family helicases suppress genome instability at G-quadruplex motifs

Katrin Paeschke[1]†*, Matthew L. Bochman[1]*, P. Daniela Garcia[1], Petr Cejka[2]†, Katherine L. Friedman[3], Stephen C. Kowalczykowski[2] & Virginia A. Zakian[1]

The *Saccharomyces cerevisiae* Pif1 helicase is the prototypical member of the Pif1 DNA helicase family, which is conserved from bacteria to humans. Here we show that exceptionally potent G-quadruplex unwinding is conserved among Pif1 helicases. Moreover, Pif1 helicases from organisms separated by more than 3 billion years of evolution suppressed DNA damage at G-quadruplex motifs in yeast. The G-quadruplex-induced damage generated in the absence of Pif1 helicases led to new genetic and epigenetic changes. Furthermore, when expressed in yeast, human PIF1 suppressed both G-quadruplex-associated DNA damage and telomere lengthening.

G-quadruplex (also known as G4) DNA is a four-stranded DNA structure held together by guanine (G) base pairing, and most genomes are replete with G4 motifs—that is, sequences that can form G4 structures *in vitro*[1]. Several DNA helicases unwind G4 structures *in vitro*, including several human helicases (WRN, BLM, FANCJ and PIF1), the mutation of which is associated with genome instability, premature ageing and/or increased cancer risk (Supplementary Table 1).

The *S. cerevisiae* 5′-to-3′ DNA helicase Pif1 has multiple nuclear functions, including inhibition of telomerase at both telomeres and double-strand breaks[2–5] and preventing replication pausing and double-stranded breaks at G4 motifs[6,7]. Unlike most eukaryotes, which encode one Pif1 helicase, *S. cerevisiae* encodes two, Pif1 and Rrm3 (ref. 8). However, Pif1 and Rrm3 have different functions. Until now, the only known nuclear functions of Rrm3 were to promote replication past stable protein complexes[9] and to separate converged replication forks[8,10]. Although the functions of human PIF1 are not known, mutation of a conserved PIF1 residue in the Pif1 family signature motif[11] is associated with increased cancer risk[12].

Pif1 is a potent G4 binder and unwinder

So far, more than 20 tested helicases, including both *S. cerevisiae* Pif1 and human PIF1, bind and/or unwind G4 structures *in vitro* (Supplementary Table 1). To determine whether *S. cerevisiae* Pif1 is particularly adept at unwinding G4 structures, we analysed its G4 binding and unwinding activities in a quantitative manner. Filter-binding assays were used to quantify Pif1 binding to different DNA substrates (Fig. 1 and Supplementary Fig. 1; oligonucleotides in Supplementary Table 2). Pif1 had a preference for poly-purine tracts (Fig. 1a), which was consistent with its preference for G-rich (dissociation constant (K_d) = 0.04 nM) over non-G-rich (K_d = 0.2 nM) single-stranded DNA (ssDNA) (Fig. 1c). Pif1 displayed similarly high binding to G4 DNA (average K_d = 0.08 nM for three G4 motifs; Fig. 1e), which was roughly 500-fold better than its binding to Y-structures (that is, Y-shaped DNA structures consisting of ssDNA arms connected to a double-stranded DNA stem) (Supplementary Fig. 1).

S. cerevisiae Pif1 efficiently unwound seven out of seven G4 substrates, six from *S. cerevisiae* chromosomal DNA and TP_{G4}, and a standard G4 substrate from the mouse immunoglobulin locus (Fig. 2a, d–f and data not shown; sequences in Supplementary Table 2). The apparent Michaelis constant (K_m) of unwinding for each G4 structure occurred at equimolar concentrations of Pif1 and the G4 substrate (0.1 nM) (Fig. 2a, d). By contrast, using the same enzyme preparation, a fivefold molar excess of Pif1 was required to unwind Y-structures (Fig. 2a), even though Y-structures are considered preferred Pif1 substrates[13].

S. cerevisiae Pif1 unwinding rates of G4 structures (Fig. 2a, d) were too fast at 30 °C to quantify. Therefore, time-course analyses were performed at a suboptimal temperature (25 °C; Fig. 2e). Even at 25 °C, Pif1 unwound 100% of the G4 substrate in 2 min. Although Pif1 cannot unwind Y-structures under single-cycle conditions[14] (that is, in the presence of a 500-fold excess of unlabelled G4 DNA), it unwound G4 structures under single-cycle conditions with no change in kinetics (Fig. 2f). Thus, G4 structures are a preferred Pif1 substrate.

Bacterial Pif1s are potent G4 unwinders

We are unable to purify full-length Rrm3, Pfh1 (the *Schizosaccharomyces pombe* Pif1 family helicase), or human PIF1 (ref. 11). However, the sequences of many bacterial Pif1 proteins are available[15]. To determine whether vigorous G4 unwinding is conserved among Pif1 family helicases, we purified Pif1 proteins from four diverse bacteria and a bacteriophage. All five enzymes robustly unwound the $rDNA_{G4}$ and TP_{G4} substrates with apparent K_m values in the subnanomolar to nanomolar range (Fig. 2d and Supplementary Fig. 2a–f). As with *S. cerevisiae* Pif1, each of these Pif1 family helicases unwound G4 DNA rapidly (Fig. 2e and Supplementary Fig. 2) and under single-cycle conditions (although not to completion) (Fig. 2c).

To determine whether a helicase is particularly good at G4 DNA unwinding, one can compare its unwinding of G4 DNA to the unwinding of other substrates (for example, *S. cerevisiae* Pif1 unwinding of G4 DNA versus Y-structures; Fig. 2a) or compare the unwinding activity of multiple helicases on the same G4 substrate. As several RecQ family helicases unwind G4 structures *in vitro* (Supplementary Table 1), we tested Sgs1, an *S. cerevisiae* RecQ helicase, and *Escherichia coli* RecQ. Sgs1 bound ssDNA and unwound Y-structures at reported rates[16] (Fig. 2b). However, Sgs1 did not bind preferentially to G-rich DNA (Fig. 1b, d), and the apparent Sgs1 binding affinity for four G4

[1]Department of Molecular Biology, Princeton University, Princeton, New Jersey 08544, USA. [2]Departments of Microbiology and Molecular Genetics, and Molecular and Cellular Biology, University of California, Davis, California 95616, USA. [3]Department of Biological Sciences, Vanderbilt University, Nashville, Tennessee 37232, USA. †Present addresses: Department of Biochemistry, Theodor Boveri-Institute, University of Würzburg, Am Hubland, D-97074 Würzburg, Germany (K.P.); Institute of Molecular Cancer Research, University of Zurich, Winterthurerstrasse 190, Zurich 8057, Switzerland (P.C.). *These authors contributed equally to this work.

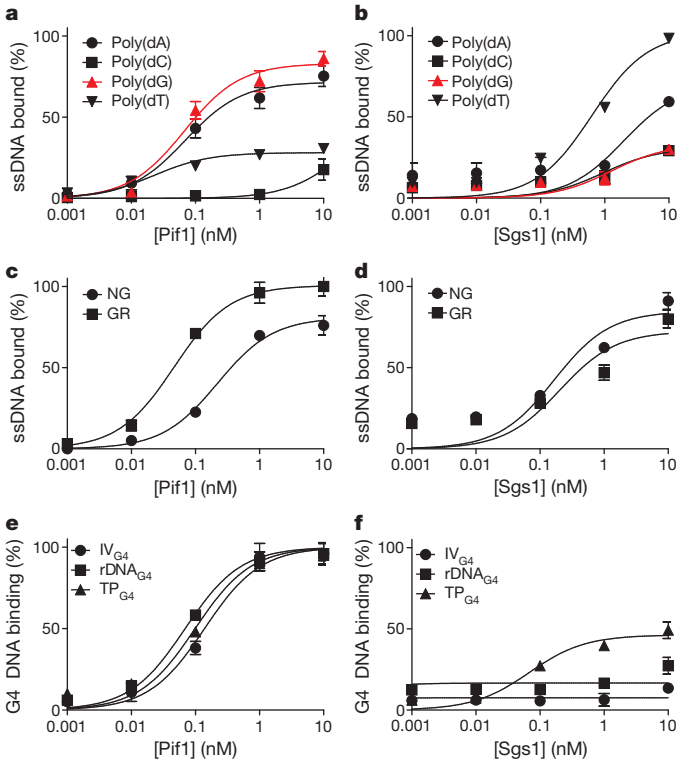

Figure 1 | Pif1 preferentially binds G4 DNA. **a**, **b**, Pif1 (**a**) and Sgs1 (**b**) binding to homopolymeric oligonucleotides. **c**, **d**, Pif1 (**c**) and Sgs1 (**d**) binding to 20-nucleotide substrates consisting of 25% each dNTP (non-G-rich, NG) or 75% purines (G-rich, GR; Supplementary Table 2). **e**, **f**, Pif1 (**e**) and Sgs1 (**f**) binding to G4 structures. Data are mean ± s.d. from ≥3 experiments.

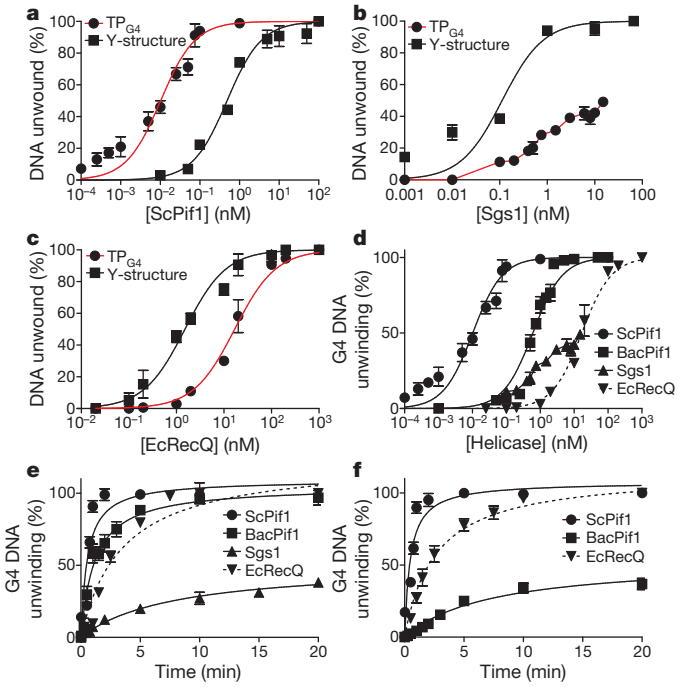

Figure 2 | Pif1 helicases preferentially unwind G4 structures. **a**–**f**, G4 and Y-structure (both 100 pM) unwinding after 20 min (or as indicated) was assessed in standard assays at 37 °C (*E. coli* RecQ (EcRecQ)), 30 °C (Sgs1, *Bacteroides* Pif1 (BacPif1)), or 25 °C (*S. cerevisiae* Pif1 (ScPif1)). A given G4 substrate differed only in the location of the poly(dA) tail (5′ for Pif1 and 3′ for RecQ). For all G4 experiments, graphs show mean unwinding by Pif1 for three G4 structures (IV$_{G4}$, rDNA$_{G4}$ and TP$_{G4}$) or TP$_{G4}$ unwinding by BacPif1, Sgs1 and RecQ. **a**–**c**, G4 and Y-structure unwinding as a function of [ScPif1] (**a**), [Sgs1] (**b**) and [EcRecQ] (**c**). **d**, G4 unwinding as a function of [helicase]. **e**, G4 unwinding time course by 100 pM ScPif1, 10 nM BacPif1, 10 nM Sgs1 and 50 nM EcRecQ. Higher Sgs1 concentrations and/or the addition of *S. cerevisiae* RPA did not increase unwinding (data not shown). **f**, G4 unwinding under single-cycle conditions by 100 pM ScPif1, 10 nM BacPif1 and 50 nM EcRecQ.

structures was more than 40-fold lower than that of *S. cerevisiae* Pif1 (Fig. 1f). Similarly, Sgs1 was considerably less efficient than all tested Pif1 family helicases at unwinding G4 structures (for example, 1,000-fold molar excess of Sgs1 was needed to unwind 50% of the G4 structures; Fig. 2e). *E. coli* RecQ displayed better unwinding of the TP$_{G4}$ substrate than Sgs1 (Fig. 2c, e, f), but the apparent K_m value of this activity was 160-fold greater than that of Pif1.

Time-course experiments revealed slower unwinding of G4 structures by Sgs1 and *E. coli* RecQ (Fig. 2e) relative to Pif1, and Sgs1 was unable to unwind G4 DNA under single-cycle conditions. Although *E. coli* RecQ did unwind the TP$_{G4}$ substrate under single-cycle conditions (Fig. 2f), 500-fold more protein relative to Pif1 was necessary for activity, yielding a half-life ($t_{1/2}$) approximately tenfold greater than that of Pif1 in the same assay. The same preparations of Sgs1 and *E. coli* RecQ unwound a conventional Y-structure 100- and 10-fold better, respectively, than G4 structures (Fig. 2b, c). With WRN, a human RecQ helicase, we obtained a similar unwinding rate for TP$_{G4}$ and rDNA$_{G4}$ as reported for TP$_{G4}$ (ref. 17); both were similar to unwinding by Sgs1 (Fig. 2e and Supplementary Fig. 3). Thus, three evolutionarily diverse RecQ helicases were much less effective than any tested Pif1 family enzyme at G4 unwinding.

Pif1s suppress G4-induced instability

We developed a quantitative assay to monitor G4-induced genome instability by modifying the gross-chromosomal rearrangement (GCR) assay[18]. The GCR assay detects complex genome rearrangements by simultaneous selection against *URA3* and *CAN1* (Fig. 3a). We modified this assay by inserting four strong Pif1-binding sites[6], two G4 motifs (Chr I$_{G4}$, Chr X$_{G4}$) and two non-G4 sites (Chr VII$_{NG}$, not G-rich; Chr I$_{GR}$, G-rich, not G4-forming; Supplementary Table 3), within the *PRB1* locus, a non-essential gene that is centromere-proximal to the two counterselectable genes (Fig. 3a). As reported[19], the GCR rate in the 'no insert' wild-type control was approximately 1×10^{-10} events per generation, and none of the inserts affected this rate (Table 1). However, the already high GCR rate in the no-insert *pif1-m2* strain was increased ~3-fold in the presence of either of the G4 motifs but was unaffected by either of the other Pif1-binding sites (Table 1). The G4 inserts did not increase GCR rates in *rrm3*Δ or *sgs1*Δ cells compared to no-insert controls. Likewise, the GCR rate in *pif1-m2 sgs1*Δ cells was not increased by the G4 inserts. However, the GCR rate in *pif1-m2 rrm3*Δ cells was approximately eight times higher in the presence of the G4 motifs compared to the *pif1-m2 rrm3*Δ strains containing no insert or non-G4 Pif1-binding sites (1,700-fold over the background no-insert wild-type levels; Table 1). These data suggest that when Pif1 levels are low, Rrm3 (but not Sgs1) suppresses G4-induced genome instability. Consistent with these findings, Rrm3 bound preferentially to G4 motifs in *pif1-m2* but not wild-type cells[20] (Supplementary Fig. 4a).

To determine whether Pif1 suppression of DNA damage at G4 motifs is evolutionarily conserved, we tested diverse Pif1 proteins for their ability to suppress the high GCR rate in *pif1-m2 rrm3*Δ+G4 cells. Helicases were introduced on a single-copy plasmid and expressed from the *RRM3* promoter (see Supplementary Fig. 6 for western analysis of protein expression). A simple spot assay was used to monitor the frequency of GCR events; cells were spotted 150 times at high density on 5-fluoroorotic acid (5-FOA) plus canavanine sulphate (Can) plates, and incubated until resistant colonies formed (~20 GCR events per spot for the *pif1-m2 rrm3*Δ+G4 strain containing no or empty vector; Fig. 4c). As expected, Pif1 and Rrm3 both suppressed the *pif1-m2 rrm3*Δ+G4 GCR rate (0.06–0.09 events per spot), whereas helicase-dead *S. cerevisiae* Pif1 (Pif1-KA) did not

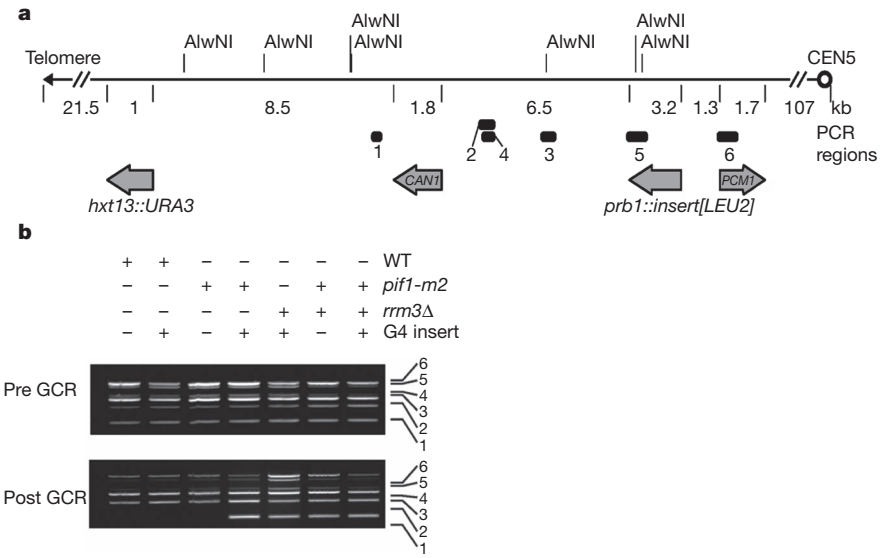

Figure 3 | Effects of G4 motifs on GCRs. **a**, Schematic of Chr. V-L in GCR strains. Numbered bars denote the positions of PCR products in **b**. *URA3* and *CAN1* denote counterselectable markers; *PCM1* is the most telomere-proximal essential gene. AlwNI sites are marked. **b**, Multiplex PCR analysis before (pre) and after (post) GCR events. Plus symbols denote that the strain was wild type (WT), had the indicated allele, and/or contained a G4 insert; minus symbols denote that the strain was not wild type, lacked the allele, and/or did not contain the G4 insert. The numbers indicate the region amplified as shown in **a**. The loss of band 1 in is consistent with telomere addition.

(19 events per spot; Fig. 4c). Remarkably, all seven heterologous Pif1 helicases, including human PIF1 (0.3 events per spot) and six prokaryotic/viral Pif1 helicases (0.07–1.0 events per spot), suppressed the high GCR rate.

Novel G4-induced events in *pif1* cells

We used several methods to determine whether G4 motifs affected the structure of the distal portion of chromosome V in the GCR events (Figs 3 and 4a, b and Supplementary Figs 4c–e and 5). As predicted[21], multiplex PCR (Fig. 3b) and Southern blot (Supplementary Fig. 4c–e) analyses revealed that almost all GCR events in the no-insert *pif1-m2* strain were due to telomere addition centromere-proximal to *CAN1* (52 out of 56 events). However, apparent telomere addition was rare (5 out of 27) or not detected (0 out of 28) in GCR clones from *pif1-m2*+G4 or *pif1-m2 rrm3*Δ+G4 cells, respectively (that is, *CAN1* fragment retained in multiplex PCR (Fig. 3b); new telomere bands were rare in Southern blots (Supplementary Fig. 4d, e)).

We also sequenced the 1,000-base-pair (bp) region around the G4 insert in individual GCR clones (Fig. 4a, b and Supplementary Fig. 5). There were no changes in this region in 17 out of 17 GCR clones from *sgs1*Δ+G4 cells. However, all (19 out of 19) G4 inserts were altered in *pif1-m2*+G4 GCR clones. These changes included mutations limited to the G4 motif (5% of clones); partial or complete deletion of the G4 motif and/or flanking DNA (10%); and more complex events involving deletions, mutations and insertions (85%) (Supplementary Fig. 5). A similar pattern was seen in most (82%) of the *pif1-m2 rrm3*Δ GCR events (Fig. 4 and Supplementary Fig. 5).

As expected, *URA3* and *CAN1* were lost or moved to new locations in all GCR clones from the wild-type strain containing a G4 insert (8 out of 8) and *sgs1*Δ+G4 (11 out of 11) cells. However, the positions of *URA3* and *CAN1* were unchanged in most *pif1-m2*+G4 (19 out of 27) and *pif1-m2 rrm3*Δ+G4 (27 out of 28) GCR clones. On the basis of the high mutation rate of the G4 inserts, we predicted that loss of *URA3* and *CAN1* expression would be due to mutations in the genes. However, cloning and sequencing of *URA3* and *CAN1* from six clones each from the *pif1-m2*+G4 and *pif1-m2 rrm3*Δ+G4 strains revealed that the *URA3* and *CAN1* sequences, including ~200 bp up and downstream of the genes, were unchanged, but the left arm of chromosome V (Chr. V-L) was unstable in many of these clones. Subsequent analyses of the same clones, for example, after restreaks or growth in liquid culture, revealed that either *URA3* or both *URA3* and *CAN1* were lost

Table 1 | Mean GCR rates

	Sequence inserted at the *PRB1* locus				
Genotype	No insert	Chr I_{G4}	Chr X_{G4}	G-rich	Non-G-rich
Wild type	1	1.2 ± 0.5	1.4 ± 0.5	1.2 ± 0.2	1.3 ± 0.6
pif1-m2	76 ± 8	200 ± 20	210 ± 10	70 ± 30	60 ± 20
*rrm3*Δ	6 ± 5	12 ± 6	9 ± 4	3 ± 1	3.2 ± 0.9
*sgs1*Δ	16 ± 5	12 ± 8	19 ± 8	ND	ND
*pif1-m2 rrm3*Δ	210 ± 32	1,500 ± 500	1,900 ± 200	200 ± 10	250 ± 40
*pif1-m2 sgs1*Δ	20 ± 80	190 ± 35	200 ± 50	ND	ND

Data are mean ± s.d. calculated from ≥3 independent experiments and normalized to the rate (1.5 (± 0.7) × 10^{-10} GCR events per generation) in the wild-type strain with no insert at the *PRB1* locus. ND, not determined.

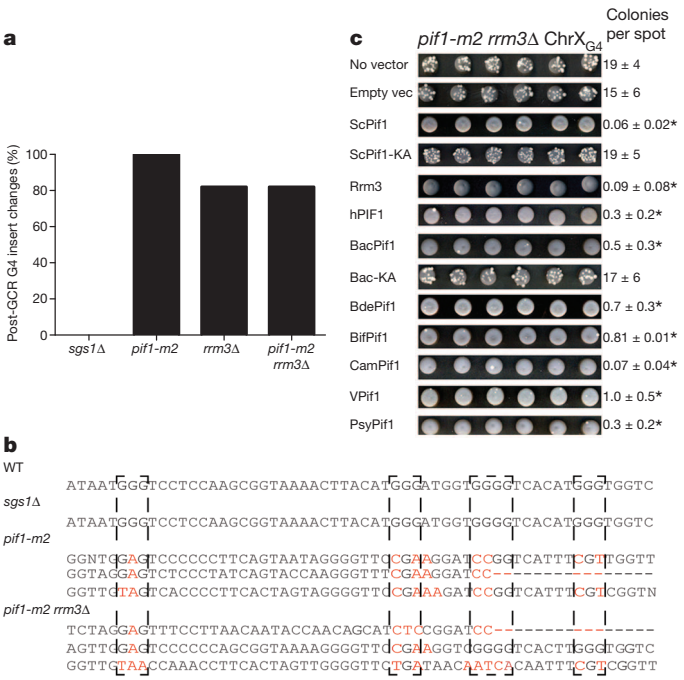

Figure 4 | Pif1 family helicases suppress G4-induced GCR events in *pif1-m2 rrm3*Δ+G4 cells. **a**, **b**, The G4-insert region was PCR-amplified and sequenced from 19 (*pif1-m2 rrm3*Δ) or 17 (others) GCR clones. **b**, Examples of G4 mutations. G-tracts involved in G4 formation are denoted by dashed boxes. Mutated G residues are in red; dashes denote deletions. **c**, GCR events in *pif1-m2 rrm3*Δ+G4 cells expressing the indicated helicase. Six out of one-hundred-and-fifty spots per strain are shown. GCR events are white colonies on a grey background of non-growing cells. The mean ± s.d. colonies per spot are indicated to the right. *$P < 0.016$ for the colonies per spot compared to the 'no vector' control as calculated by Student's *t*-test. BdePif1, *Bdellovibrio* Pif1; BifPif1, *Bifidobacterium* Pif1; CamPif1, *Campylobacter* Pif1; hPIF1, human PIF1; PsyPif1, *Psychrobacter* Pif1; VPif1, V99B1Pif1.

as often as 95% of the time (data not shown). However, some clones maintained wild-type *URA3* and *CAN1* genes for ≥200 generations.

Mechanism of G4-induced silencing

Given that the sequences and positions of *URA3* and *CAN1* were unchanged in the *pif1-m2*+G4, *pif1-m2 rrm3*Δ+G4 and *pif1-m2 rrm3*Δ GCR clones that retained these genes, their 5-FOA- and Can-resistant (FOA^R Can^R) phenotypes must be due to epigenetic silencing. To determine whether the silencing occurred at the transcriptional level, we used real-time quantitative PCR (qPCR) to assess the amounts of *URA3* and *CAN1* messenger RNA in four independent *pif1-m2 rrm3*Δ+G4 GCR clones and the parental pre-GCR strain. Depending on the clone, *URA3* mRNA levels ranged from 9 to 24% of the levels in the pre-GCR strain; *CAN1* mRNA ranged from 20 to 53% of the control in the same clones (Fig. 5a, b). Thus, silencing was not due to translational regulation.

In many organisms, including *S. cerevisiae* and humans[22,23], genes that are near telomeres are transcriptionally repressed (telomere position effect (TPE); reviewed in ref. 24). To determine whether the silencing observed in the *pif1-m2*+G4 GCR clones was due to TPE, we deleted *SIR2*, which encodes a protein that is required for TPE, in two independent *pif1-m2*+G4 GCR clones that retained *URA3* and *CAN1* in their original positions. Both clones lost their FOA^R Can^R phenotypes, suggesting that silencing was due to a TPE-like mechanism.

Human PIF1 inhibits telomere lengthening

Telomeres are longer in Pif1-deficient cells owing to the ability of *S. cerevisiae* Pif1 to remove telomerase from DNA ends[2,3]. To determine whether other Pif1 helicases inhibit yeast telomerase, we determined telomere length in *pif1-m2* cells expressing heterologous Pif1 helicases (Fig. 5c). Empty vector or the expression of bacterial Pif1s (*Bacteroides* Pif1 and *Campylobacter* Pif1) or *S. pombe* Pfh1 did not suppress the long telomere phenotype of *pif1-m2* cells. Indeed, telomeres were even longer in *pif1-m2* cells expressing bacterial Pif1s or Pfh1 than in *pif1-m2* cells alone. However, human PIF1 was nearly as effective as *S. cerevisiae* Pif1 in restoring telomere length to *pif1-m2* cells (Fig. 5c), even though it was expressed at much lower levels (Supplementary Fig. 6).

Discussion

S. cerevisiae Pif1 and five prokaryotic Pif1 helicases were extremely proficient at unwinding G4 structures (Fig. 2 and Supplementary Fig. 2), whereas three RecQ helicases had ~1,000-fold lower G4 unwinding activity than the Pif1 helicases (Fig. 2 and Supplementary Figs 2 and 3). Moreover, although *S. cerevisiae* Pif1 unwound G4 structures much better than Y-structures (Fig. 2a), which are themselves a preferred Pif1 substrate[13], Sgs1 and *E. coli* RecQ were more active on Y-structure than G4 substrates (Fig. 2b, c). Thus, vigorous G4 unwinding is a conserved feature of Pif1 helicases.

Suppression of G4-induced DNA instability was also conserved (Table 1). In *pif1-m2* cells, GCR rates were increased when the substrate contained a G4 motif but not when it contained other strong Pif1-binding sites; this effect is probably underestimated as *pif1-m2* is not a null allele[3]. Similarly, the human minisatellite CEB1, a tandem array of ~40 [GC]-rich repeats, increases the GCR rate in *pif1*Δ cells[25]. In contrast to no-insert *pif1-m2* cells, G4-mediated GCR events were rarely due to telomere addition (52 telomere additions per 56 GCR events in *pif1-m2* cells, versus 5 telomere additions per 27 GCR events in *pif1-m2*+G4 cells). In both *pif1-m2* and *pif1-m2 rrm3*Δ cells, the G4-induced events were usually associated with mutation of the G4 insert so that it could no longer form a G4 structure (Fig. 4a), suggesting that the process enabling cells to replicate and/or repair a G4 motif in the absence of Pif1 helicases is error-prone. Remarkably, the double drug-resistant phenotype of the G4-induced clones recovered from *pif1-m2*+G4 (75 out of 104 clones) and *pif1-m2 rrm3*Δ+G4 (50 out of 64 clones) cells was usually due to epigenetic silencing, although the genes could be lost during further outgrowth. Although silencing of *URA3* and *CAN1* in these complex genetic-epigenetic (CGE) clones was Sir2-dependent, as is TPE[26], this silencing was considerably more effective than classical TPE. When *URA3* is immediately adjacent to the chromosome VII-L telomere, mRNA levels are ~20% of control levels, but when *URA3* is ~20 kilobases (kb) from the same telomere, FOA^R colonies are not detected ($<6\times10^{-7}$). By contrast, in CGE clones, the average *URA3* mRNA level was 19% of the control, even though *URA3* was 21 kb from the telomere. The extension of silencing to more internal sites may be associated with impaired replication through a G4 structure, as changes in silencing occur in translesion polymerase-defective avian DT40 cells[27]. The unusual *URA3* and *CAN1* silencing seen here also required or was enhanced by lack of Pif1 and/or Rrm3, as it was not detected in *sgs1*Δ+G4 GCR clones (0 out of 17 clones). Furthermore, it was enhanced by a nearby G4 motif as it was not seen in GCR clones from the no-insert *pif1-m2* cells (0 out of 56 clones). The new events at both G4 motifs and structural genes in the absence of Pif1 family helicases are distinct from previously described GCR events. Thus, we term them CGE events. The epigenetic silencing of *URA3* and *CAN1* is reminiscent of the gene silencing that occurs in some human tumours that can lead to loss of heterozygosity.

Although Pif1 and Rrm3 have largely non-overlapping functions[11], they both suppressed damage at G4 motifs, as did seven out of seven heterologous Pif1 helicases (Fig. 4c). This suppression was efficient. For example, human PIF1 suppressed CGE events ~20% as effectively as *S. cerevisiae* Pif1, even though it was expressed at considerably lower

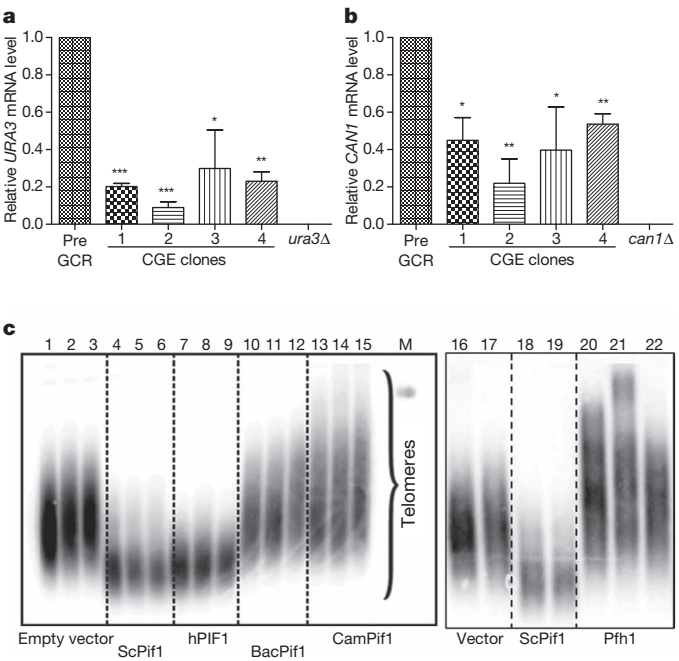

Figure 5 | Mechanism of CGE silencing and effect of Pif1 helicases on telomere length. **a**, **b**, *URA3* (**a**) and *CAN1* (**b**) mRNA levels in *pif1-m2 rrm3*Δ+G4 CGE clones and controls (pre-GCR parental strains and *ura3*Δ and *can1*Δ cells). Quantitative reverse-transcriptase PCR (qRT–PCR) was used to determine the *ACT1*, *URA3* or *CAN1* mRNA levels in the indicated strains. *URA3* and *CAN1* values were normalized to *ACT1* levels in each strain; the $2^{-\Delta\Delta Ct}$ method[38] was used to determine *URA3* and *CAN1* levels relative to parental pre-GCR cells. $*P<0.05$; $**P<0.01$; $***P<0.001$. **c**, Telomere blot of DNA from *pif1-m2* spore clones expressing vector only (lanes 1–3, 16, 17), ScPif1 (lanes 4–6, 18, 19), human PIF1 (7–9), two different bacterial Pif1s (10–12, 13–15), or Pfh1 (20–22). M, markers. DNA was prepared ~50, 75 and 100 generations after sporulation (first, second and third lanes in each set) or 100 generations after sporulation from two or three spore clones (lanes 16–22). See Supplementary Fig. 7 for full gel images.

levels (Supplementary Fig. 6). Thus, activity at G4 DNA by both *in vitro* and *in vivo* assays is a conserved feature of Pif1 family helicases.

S. cerevisiae Pif1 (but not Rrm3 or Pfh1) inhibits telomerase[4,28,29]. Human PIF1 (but not prokaryotic Pif1 helicases or Pfh1) restored telomere length in *pif1-m2* cells (Fig. 5c), suggesting that PIF1 is a regulator of both telomerase and G4 structures in its endogenous context. One or both of these activities might explain why mutation of human PIF1 is associated with cancer[12].

METHODS SUMMARY

Strains were YPH500 (ref. 30) derivatives (Supplementary Tables 4 and 5). Cloning oligonucleotides are listed in Supplementary Table 6. The *pif1-m2* allele was used instead of *pif1*Δ because *pif1-m2* cells are mitochondrial proficient and grow at near-wild-type rates[3]. Pif1, Sgs1 and *E. coli* RecQ were purified and assayed as described[14,16,31]. Bacterial Pif1 helicases were cloned (Supplementary Table 8), overexpressed and purified as described in the Methods. G4 motifs were from the yeast genome[32] or mouse immunoglobulin locus (TP_{G4}) (Supplementary Tables 2 and 3). G4 structures were formed *in vitro*[33] and 5′-end labelled with [γ-^{32}P]ATP. Protein–DNA binding was analysed by the double-filter binding method[34]. Activity of all Pif1 enzymes was measured as described previously[14]. WRN helicase assays were as described[35]. GCR assays were performed as described[36]. GCR rates were calculated using the FALCOR web server and MMS maximum likelihood method[37]. Multiplex PCR oligonucleotides are in Supplementary Table 7. G4 inserts were sequenced from genomic DNA and analysed with Biology WorkBench tools (http://workbench.sdsc.edu/). Suppression analyses of GCR phenotypes were performed in *pif1-m2 rrm3*Δ+G4 cells carrying a single-copy *TRP1*-marked plasmid with 3×Flag-tagged helicase genes under control of the *RRM3* promoter (Supplementary Table 8). Chromatin immunoprecipitation was performed as described previously[6,20]. Total RNA was isolated using a Quick-RNA MiniPrep kit (Zymo Research), reverse-translated into complementary DNA using an iScript One-Step RT–PCR kit with SYBR Green (Bio-Rad), and analysed by real-time PCR using a Bio-Rad CFX96 real-time system.

Full Methods and any associated references are available in the online version of the paper.

Received 6 August 2012; accepted 5 April 2013.
Published online 8 May 2013.

1. Bochman, M. L., Paeschke, K. & Zakian, V. A. DNA secondary structures: stability and function of G-quadruplex structures. *Nature Rev. Genet.* **13,** 770–780 (2012).
2. Boulé, J.-B., Vega, L. & Zakian, V. The Yeast Pif1p helicase removes telomerase from DNA. *Nature* **438,** 57–61 (2005).
3. Schulz, V. P. & Zakian, V. A. The *Saccharomyces PIF1* DNA helicase inhibits telomere elongation and *de novo* telomere formation. *Cell* **76,** 145–155 (1994).
4. Zhou, J.-Q., Monson, E. M., Teng, S.-C., Schulz, V. P. & Zakian, V. A. The Pif1p helicase, a catalytic inhibitor of telomerase lengthening of yeast telomeres. *Science* **289,** 771–774 (2000).
5. Myung, K., Chen, C. & Kolodner, R. D. Multiple pathways cooperate in the suppression of genome instability in *Saccharomyces cerevisiae*. *Nature* **411,** 1073–1076 (2001).
6. Paeschke, K., Capra, J. A. & Zakian, V. A. DNA replication through G–quadruplex motifs Is promoted by the *Saccharomyces cerevisiae* Pif1 DNA helicase. *Cell* **145,** 678–691 (2011).
7. Lopes, J. *et al.* G–quadruplex-induced instability during leading-strand replication. *EMBO J.* **30,** 4033–4046 (2011).
8. Ivessa, A. S., Zhou, J.-Q. & Zakian, V. A. The *Saccharomyces* Pif1p DNA helicase and the highly related Rrm3p have opposite effects on replication fork progression in ribosomal DNA. *Cell* **100,** 479–489 (2000).
9. Ivessa, A. S. *et al.* The *Saccharomyces cerevisiae* helicase Rrm3p facilitates replication past nonhistone protein-DNA complexes. *Mol. Cell* **12,** 1525–1536 (2003).
10. Fachinetti, D. *et al.* Replication termination at eukaryotic chromosomes is mediated by Top2 and occurs at genomic loci containing pausing elements. *Mol. Cell* **39,** 595–605 (2010).
11. Bochman, M. L., Sabouri, N. & Zakian, V. A. Unwinding the functions of the Pif1 family helicases. *DNA Repair (Amst.)* **9,** 237–249 (2010).
12. Chisholm, K. M. *et al.* A genomewide screen for suppressors of *Alu*-mediated rearrangements reveals a role for PIF1. *PLoS ONE* **7,** e30748 (2012).
13. Lahaye, A., Leterme, S. & Foury, F. PIF1 DNA helicase from *Saccharomyces cerevisiae*. Biochemical characterization of the enzyme. *J. Biol. Chem.* **268,** 26155–26161 (1993).
14. Boulé, J. B. & Zakian, V. A. The yeast Pif1p DNA helicase preferentially unwinds RNA DNA substrates. *Nucleic Acids Res.* **35,** 5809–5818 (2007).
15. Bochman, M. L., Judge, C. P. & Zakian, V. A. The Pif1 family in prokaryotes: what are our helicases doing in your bacteria? *Mol. Biol. Cell* **22,** 1955–1959 (2011).
16. Cejka, P. & Kowalczykowski, S. C. The full-length *Saccharomyces cerevisiae* Sgs1 protein is a vigorous DNA helicase that preferentially unwinds holliday junctions. *J. Biol. Chem.* **285,** 8290–8301 (2010).
17. Mohaghegh, P., Karow, J. K., Brosh Jr, R. M., Bohr Jr, V. A. & Hickson, I. D. The Bloom's and Werne's syndrome proteins are DNA structure-specific helicases. *Nucleic Acids Res.* **29,** 2843–2849 (2001).
18. Schmidt, K. H., Pennaneach, V., Putnam, C. D. & Kolodner, R. D. Analysis of gross-chromosomal rearrangements in *Saccharomyces cerevisiae*. *Methods Enzymol.* **409,** 462–476 (2006).
19. Chen, C. & Kolodner, R. D. Gross chromosomal rearrangements in *Saccharomyces cerevisiae* replication and recombination defective mutants. *Nature Genet.* **23,** 81–85 (1999).
20. Azvolinsky, A., Giresi, P., Lieb, J. & Zakian, V. Highly transcribed RNA polymerase II genes are impediments to replication fork progression in *Saccharomyces cerevisiae*. *Mol. Cell* **34,** 722–734 (2009).
21. Smith, S. *et al.* Mutator genes for suppression of gross chromosomal rearrangements identified by a genome-wide screening in *Saccharomyces cerevisiae*. *Proc. Natl Acad. Sci. USA* **101,** 9039–9044 (2004).
22. Gottschling, D. E., Aparicio, O. M., Billington, B. L. & Zakian, V. A. Position effect at *S. cerevisiae* telomeres: reversible repression of Pol II transcription. *Cell* **63,** 751–762 (1990).
23. Baur, J. A., Zou, Y., Shay, J. W. & Wright, W. E. Telomere position effect in human cells. *Science* **292,** 2075–2077 (2001).
24. Mondoux, M. & Zakian, V. in *Telomeres* 2nd edn (eds de Lange, T., Lundblad, V. & Blackburn, E. H.) 261–316 (CSHL, 2005).
25. Piazza, A. *et al.* Stimulation of gross chromosomal rearrangements by the human CEB1 and CEB25 minisatellites in *Saccharomyces cerevisiae* depends on G-quadruplexes or Cdc13. *PLoS Genet.* **8,** e1003033 (2012).
26. Aparicio, O. M., Billington, B. L. & Gottschling, D. E. Modifiers of position effect are shared between telomeric and silent mating-type loci in *S. cerevisiae*. *Cell* **66,** 1279–1287 (1991).
27. Sarkies, P., Reams, C., Simpson, L. J. & Sale, J. E. Epigenetic instability due to defective replication of structured DNA. *Mol. Cell* **40,** 703–713 (2010).
28. Ivessa, A. S., Zhou, J.-Q., Schulz, V. P., Monson, E. M. & Zakian, V. A. *Saccharomyces* Rrm3p, a 5′ to 3′ DNA helicase that promotes replication fork progression through telomeric and sub-telomeric DNA. *Genes Dev.* **16,** 1383–1396 (2002).
29. Pinter, S. F., Aubert, S. D. & Zakian, V. A. The *Schizosaccharomyces pombe* Pfh1p DNA helicase is essential for the maintenance of nuclear and mitochondrial DNA. *Mol. Cell. Biol.* **28,** 6594–6608 (2008).
30. Sikorski, R. S. & Hieter, P. A system of shuttle vectors and yeast host strains designed for efficient manipulation of DNA in *Saccharomyces cerevisiae*. *Genetics* **122,** 19–27 (1989).
31. Harmon, F. G. & Kowalczykowski, S. C. RecQ helicase, in concert with RecA and SSB proteins, initiates and disrupts DNA recombination. *Genes Dev.* **12,** 1134–1144 (1998).
32. Capra, J. A., Paeschke, K., Singh, M. & Zakian, V. A. G-quadruplex DNA sequences are evolutionarily conserved and associated with distinct genomic features in *Saccharomyces cerevisiae*. *PLOS Comput. Biol.* **6,** e1000861 (2010).
33. Bachrati, C. Z. & Hickson, I. D. Analysis of the DNA unwinding activity of RecQ family helicases. *Methods Enzymol.* **409,** 86–100 (2006).
34. Wong, I. & Lohman, T. M. A double-filter method for nitrocellulose-filter binding: application to protein-nucleic acid interactions. *Proc. Natl Acad. Sci. USA* **90,** 5428–5432 (1993).
35. Brosh, R. M. Jr, Opresko, P. L. & Bohr, V. A. Enzymatic mechanism of the WRN helicase/nuclease. *Methods Enzymol.* **409,** 52–85 (2006).
36. Putnam, C. D. & Kolodner, R. D. Determination of gross chromosomal rearrangement rates. *Cold Spring Harbor Protoc.* **2010,** pdb.prot5492 (2010).
37. Hall, B. M., Ma, C. X., Liang, P. & Singh, K. K. Fluctuation analysis CalculatOR: a web tool for the determination of mutation rate using Luria–Delbruck fluctuation analysis. *Bioinformatics* **25,** 1564–1565 (2009).
38. Heid, C. A., Stevens, J., Livak, K. J. & Williams, P. M. Real time quantitative PCR. *Genome Res.* **6,** 986–994 (1996).

Supplementary Information is available in the online version of the paper.

Acknowledgements We thank J. B. Boule for early work on *S. cerevisiae* Pif1 biochemistry, P. Opresko for the gift of purified human WRN, E. Allen-Vercoe, K. Bidle, C. Parker, R. Johnson, H. L. Ayala-del-Rio and E. Sockett for materials and for cloning non-yeast Pif1 helicases, and M. Platts for multiplex PCR and Southern analysis methods to characterize GCR clones. We acknowledge financial support from the National Institutes of Health (V.A.Z., S.C.K.), National Science Foundation (K.L.F.), DFG and NJCCR (K.P.) and American Cancer Society (M.L.B.).

Author Contributions K.P. and M.L.B. purified Pif1 helicases and performed biochemical and GCR experiments; P.D.G. and M.L.B. did the silencing experiments; P.C. purified Sgs1; S.C.K. aided in the analysis and interpretation of the biochemistry and provided purified *E. coli* RecQ; K.L.F. aided in the analysis and interpretation of GCR events; K.P., M.L.B. and V.A.Z. designed the study, analysed data and wrote the manuscript. K.P. and M.L.B. contributed equally. All authors discussed the results and commented on the manuscript.

Author Information Reprints and permissions information is available at www.nature.com/reprints. The authors declare no competing financial interests. Readers are welcome to comment on the online version of the paper. Correspondence and requests for materials should be addressed to V.A.Z. (vzakian@princeton.edu).

METHODS

Methods Summary. Strains were YPH500 (ref. 30) derivatives (Supplementary Tables 4 and 5). *E. coli* RecQ was purified and assayed as described[31]. G4 motifs were from the yeast genome[32] or mouse immunoglobulin locus (TP_{G4}) (Supplementary Tables 2 and 3). G4 structures were formed *in vitro*[33] and 5′-end labelled with [γ-^{32}P]ATP. Protein–DNA binding was analysed by the double-filter binding method[34]. WRN helicase assays were as described[35]. GCR assays were performed as described[36]. GCR rates were calculated using the FALCOR web server and MMS maximum likelihood method[37].

Yeast strains. All experiments were performed in the YPH500 background[30]. Yeast strains are listed in Supplementary Table 4, except for those used in the GCR assays (Supplementary Table 5). Gene disruptions and epitope tagging of proteins were confirmed by colony PCR, sequencing, Southern blotting and/or phenotypic analysis. The *pif1-m2* allele was introduced as previously described[3] (see Supplementary Table 6 for oligonucleotide sequences used for cloning). The carboxy terminus of Rrm3 was tagged at its endogenous locus with 13 Myc epitopes using PCR[39]. Tagged Rrm3 was expressed from its own promoter as the only version of the protein in the strain. Plasmids are listed in Supplementary Table 8. All GCR strains (Supplementary Table 5) are derivatives of YPH500 in which *HXT13* was deleted with the *Kluyveromyces lactis URA3* gene using pUG72 (ref. 40) and oligonucleotides MB262 and MB277 (see Supplementary Table 6 for the sequences of oligonucleotides used in GCR strain construction). The partial loss of nuclear function *pif1-m2* allele was used instead of *pif1*Δ because *pif1-m2* cells are mitochondrial proficient[3]. *RRM3* was deleted with *HIS3MX6* using pFA6a-His3MX6 (ref. 41) and oligonucleotides MB30 and MB31. *SGS1* was deleted with the *S. pombe his5*$^{+}$ gene using pUG27 (ref. 40) and oligonucleotides MB32 and MB33 (Supplementary Table 6). Strains containing 'inserts' (Supplementary Table 5) were made by deleting *PRB1* with *LEU2* marked cassettes using oligonucleotides KP321f and KP321r (Supplementary Table 8). The *LEU2* marked cassettes were derived from pRS415-based plasmids[30] containing the designated inserts cloned into the XbaI and BamHI sites (Supplementary Table 8).

Biochemical methods. Full-length *S. cerevisiae* Pif1 and Sgs1 and *E. coli* RecQ were purified as previously described[14,16,31]. *In vitro* analyses of independent protein preparations revealed little to no prep-to-prep variability and that these preparations had similar biochemical activities (that is, ssDNA binding and Y-structure DNA unwinding, see below) to previously published values[14,16,31].

Bacterial Pif1 helicases were cloned as follows. E. Allen-Vercoe, C. Parker, R. Johnson and H. L. Ayala-del-Rio provided genomic DNA from *Bacteroides* sp. 2_1_16, *Campylobacter jejuni* subsp. jejuni NCTC 11168, *E. coli* phage rv5 and *Psychrobacter* sp. PRwf-1, respectively. A pUC19-based plasmid containing the gene encoding the *Bdellovibrio bacteriovorus* HD100 Pif1 helicase (Supplementary Table 8) was a gift from E. Sockett. PCR primers were designed to amplify the Pif1-like helicase genes from the above mentioned organisms (see Supplementary Table 6) with iProof HF Master Mix (BioRad). PCR products were then digested and ligated into a modified pET21d vector (pMB116; Supplementary Table 8) such that they were in-frame with an amino-terminal 4× Strep-tag II sequence and a C-terminal 6× His tag. Additional cloning details and nucleotide sequences are available on request.

Expression plasmids were transformed into Rosetta 2(DE3) pLysS cells and selected for at 37 °C on Luria–Bertani (LB) medium supplemented with 100 μg ml^{-1} ampicillin and 34 μg ml^{-1} chloramphenicol. Fresh transformants were used to inoculate one or more 5-ml LB cultures supplemented with antibiotics and incubated at 30 °C for ~6 h with agitation. These starter cultures were then diluted 1:100 in ZYP-5052 auto-induction medium containing 1× trace metals mix[42], 100 μg ml^{-1} ampicillin and 34 μg ml^{-1} chloramphenicol, and incubated at 30 °C with agitation to attenuance (*D*) at 600 nm of >3 (~18 h). Cells were collected by centrifugation for 10 min in a GS-3 rotor at 4,225*g* and 4 °C. Cell pellets were weighed and frozen at −80 °C before lysis or for long-term storage.

The cells were thawed at room temperature and resuspended in 2 ml g^{-1} cell pellet buffer A (50 mM Na-HEPES, pH 8, 10% (v/v) glycerol, 300 mM NaCl and 5 mM $MgCl_2$) supplemented with 1× protease inhibitor cocktail (Sigma), 20 μg ml^{-1} DNase I, and 2.5 μg ml^{-1} RNase A. Cells were lysed for 10 min at room temperature by adding methyl-6-*O*-(*N*-heptylcarbamoyl)-α-D-glucopyranoside (HECAMEG; Sigma) to a final concentration of 0.05% (w/v) and 1× BugBuster (Novagen) or FastBreak (Promega) with gentle stirring. Subsequent steps were performed at 4 °C.

The soluble fraction was clarified by centrifugation for 30 min in an SA-600 rotor at 20,200*g* followed by filtering the supernatant through a 0.22-μm membrane. This mixture was then loaded onto a Strep-Tactin Sepharose gravity column (IBA) pre-equilibrated in buffer A. The column was washed with four column volumes each of buffer W1 (50 mM Na-HEPES, pH 8, 10% (v/v) glycerol, 500 mM NaCl, 5 mM $MgCl_2$ and 0.05% (v/v) HECAMEG), W2 (50 mM Na-HEPES, pH 8, 10% (v/v) glycerol, 300 mM NaCl, 5 mM $MgCl_2$, 0.05% (v/v) HECAMEG and 5 mM ATP), and W3 (50 mM Na-HEPES, pH 8, 10% (v/v) glycerol, 300 mM NaCl, 5 mM $MgCl_2$ and 0.01% (v/v) HECAMEG). Protein was eluted with three column volumes of buffer W3 supplemented with 1 mM desthiobiotin. Column fractions were examined on 10% SDS–PAGE gels run at 20 V cm^{-1} and stained with Coomassie blue R-250 (BioRad).

Peak fractions were pooled and loaded onto a His60 Ni gravity column (Clontech) pre-equilibrated in buffer W3. The column was washed with five column volumes of buffer W3 supplemented with 25 mM imidazole, and protein was eluted with five column volumes of W3 supplemented with 250 mM imidazole. Fractions were analysed by SDS–PAGE as above, and peak fractions were pooled and extensively dialysed against storage buffer (50 mM Na-HEPES, pH 8, 30% (v/v) glycerol, 50 mM NaCl, 150 mM sodium acetate, pH 7.6, 25 mM $(NH_4)_2SO_4$, 5 mM magnesium acetate, 1 mM dithiothreitol and 0.01% (v/v) HECAMEG) using 30-kilodalton (kDa) (Slide-A-Lyzer; Pierce) or 50-kDa (Tube-O-DIALYZER; G-Biosciences) molecular mass cut-off membranes. Protein concentration and purity in the final dialysates were determined on SYPRO orange (Sigma)-stained SDS–PAGE gels using known amounts of a standard protein for comparison. In all cases, protein purity was ≥95%.

For some protein preparations, the N-terminal 4× Strep-II tag was removed by PreScission Protease (GE Healthcare) digestion (2 U protease per ml protein at 4 °C overnight) before His60 column chromatography. In all cases, removal of the tag had little effect on subsequent protein purity and no effect on the *in vitro* activities examined. However, tag cleavage occasionally resulted in precipitation of a considerable portion of the protein. Thus, recombinant proteins containing both N- and C-terminal tags were used for all experiments shown.

For preparation of substrates, various *S. cerevisiae* G4 motifs were chosen from the >500 identified G4 motifs in the budding yeast genome[32] (see Supplementary Tables 2 and 3 for sequences). Oligonucleotides of G4 motifs were synthesized by IDT. The concentrations of all oligonucleotides were estimated using extinction coefficients provided by the manufacturer. G4 DNA structures were formed *in vitro* as described[33]. Formation of G4 structures was confirmed by non-denaturing PAGE. After G4 structure formation, the substrates were 5′-labelled with T4 polynucleotide kinase (NEB) and [γ-^{32}P]ATP, purified by 7% non-denaturing PAGE, and visualized using phosphoimaging.

In all biochemical assays, 100 pM radioactively labelled DNA was used, unless noted otherwise, and the reaction buffers used were previously described for *S. cerevisiae* Pif1 (ref. 14) Sgs1 (ref. 16) and *E. coli* RecQ[31]. In brief, protein–DNA binding was analysed using a BioDot SF apparatus (Bio-Rad) by the double-filter binding method[34]. Reactions were set up as for helicase assays, but ATP was omitted. The reactions were incubated on ice for 30 min, filtered through the membranes, and then the membranes were washed with additional reaction buffer. The membranes were dried and analysed by phosphoimaging. Pif1, Sgs1 and RecQ helicase activity assays were performed essentially as described previously[14,16,31]. The helicase activity of non-yeast Pif1 enzymes was also measured as described for *S. cerevisiae* Pif1 previously[14]. WRN helicase assays were performed as described[35]. For protein titrations, reactions were incubated for 30 min at helicase at 25 °C Pif1), 30 °C (Sgs1), or 37 °C (RecQ, WRN, and non-yeast Pif1). In time-course experiments, 100 pM ScPif1, 10 nM BacPif1, 10 nM Sgs1 or 50 nM EcRecQ was added to the reaction; 100 pM Sgs1 or EcRecQ displayed only basal levels of unwinding in our G4 unwinding assays. For single-cycle conditions, we used a 500× excess of either G4 DNA or ssDNA as a protein trap. The excess trap DNA was added together with ATP to start the reactions.

The data were fit with rectangular hyperbolic curves using GraphPad Prism 5 and equation (1):

$$Y = \frac{B_{max} \cdot X}{K + X} \quad (1)$$

in which X is the helicase concentration or time (as indicated), Y is either DNA binding or unwinding (as indicated), B_{max} is the maximum level of binding or unwinding (as indicated), and K is the midpoint of the curve. When a $\log_{10}$-scale x axis is used, the hyperbolic curve assumes a sigmoidal shape.

GCR assays. GCR assays were cloned and performed essentially as described[36] (primer sequences for cloning are listed in Supplementary Table 6). In brief, sets of five or more 5-ml cultures of each *S. cerevisiae* GCR strain (Supplementary Table 5) were grown to saturation in YPD medium at 30 °C for 36–48 h. A final dilution of 1×10^{-7} of each culture was plated on YPD and incubated at room temperature for 4 days to determine the viable cell count. Cells (1.5 or 2 ml) from each culture were pelleted, resuspended in sterile water, plated on drop-out medium lacking uracil and arginine (US Biologicals) supplemented with 1 g l^{-1} 5-FOA and 60 mg l^{-1} canavanine sulphate (FOA+Can), and incubated at 30 °C for ~4 days. GCR rates were calculated using the FALCOR web server and MMS maximum likelihood method[37] and normalized to wild-type rate of 10^{-10} GCR events per cell division. The rates presented in Table 1 are the mean ± s.d. of

≥3 experiments per strain. We define GCR clones as colonies that grew on the FOA+Can plates. Such FOA- and Can-resistant (FOA^R Can^R) clones were selected for post-GCR analyses (below).

G4 inserts were sequenced from samples of genomic DNA from FOA^R Can^R clones prepared using a MasterPure Yeast DNA Purification kit (Epicentre) following the manufacturer's instructions. The oligonucleotides used for sequencing the Watson and Crick strands are: MB540, 5′-CAATAGGCCGAAA TCGGCAAAATCCC-3′, and MB537, 5′-CTCCTATGTTGTGTGGAATTG TGAGCGG-3′, respectively, which amplified a ~1-kb region containing the inserts. The results were analysed using the Biology WorkBench tools (http://workbench.sdsc.edu/) and classified into four different categories, as indicated in Supplementary Fig. 5: (1) no change, the G4 inserts were identical to the starting strain in the GCR clones; (2) recombination, the G4 insert was replaced with a partially homologous sequence from chromsome VII; (3) mutation and deletion, several of the guanines responsible for forming the G4 structures were either mutated to other residues or deleted; and (4) mutation/deletion/insertion, the G4 inserts experienced a variety of events, including substitution mutations and short deletions and/or insertions.

Suppression analyses of the *pif1-m2 rrm3*Δ+G4 GCR phenotype were performed by transforming strain KP326 (Supplementary Table 5) with *TRP1*-marked plasmids containing C-terminally 3× Flag-tagged helicase genes expressed under control of the *RRM3* promoter (Supplementary Table 8). Three independent colonies were used to inoculate 5 ml synthetic complete medium lacking tryptophan (SC−Trp) and grown on a roller drum for ~48 h at 30 °C. The $D_{660\,nm}$ for each culture was determined with a spectrophotometer, and the cells were pelleted by centrifugation and resuspended to $D_{660\,nm} = 10$ in sterile H_2O. Then, a repeat pipettor was used to spot 10-µl samples of each strain 50 times on a FOA+Can plate, and the plates were incubated at 30 °C for 4 days. This process was repeated ≥3 times for each strain. When colonies appeared on the FOA+Can plates, the number of colonies per 10-µl spot was counted, and the average number of colonies in the 50 spots per plate was calculated. The mean (± s.d.) of these values from the ≥3 plates per strain was determined and reported in the right column of Fig. 4c.

Western and Southern blotting. Cell extracts for western blotting were prepared as described previously[43]. In brief, cells were grown overnight in SC−Trp liquid medium at 30 °C with aeration. Then, 1 ml of $D_{600\,nm} = 2.5$ cells was collected, resuspended in 200 µl 0.1 N NaOH, incubated at room temperature for 5 min, pelleted, resuspended in 50 µl SDS–PAGE sample buffer, boiled for 3 min, and pelleted again. Subsequently, 6 µl of the supernatants was loaded onto an 8% (37.5:1 polyacrylamide:bis-acrylamide) SDS–PAGE gel and run at 20 V cm^{-1}. The proteins were transferred to a nitrocellulose membrane at 4 °C and blocked with 5% non-fat milk in TBST at room temperature using standard protocols. The blot was probed with a monoclonal anti-Flag antibody (F1804, Sigma) and visualized with a horseradish peroxidase (HRP)-conjugated secondary antibody and ECL detection reagents (GE Healthcare). The blot was then stripped and reprobed with an anti-tubulin antibody (G094, ABM) to verify equivalent protein loading.

For telomere blots, cells containing a plasmid with either a helicase gene (pMB267, 270, 282 and 292) or no insert (empty vector control; pMB13) (Supplementary Table 8) were transformed into the *PIF1 pif1-m2* diploid (KP448). The diploids were sporulated, and the *pif1-m2* spore clones carrying the plasmids were recovered. Genomic DNA was isolated from cells from restreaks 1–6 after sporulation (corresponding to approximately 25 generations per restreak) using a MasterPure Yeast DNA Isolation kit (Epicentre Biotechnologies), digested overnight with PstI and XhoI (NEB), and telomere length was determined by Southern analysis as described previously[44]. Results from DNA from restreaks 1–3 are shown in Fig. 5d, but the same results were also observed after 6 restreaks.

When colonies arose after GCR events, single colonies were restreaked onto FOA+Can plates, and genomic DNA was isolated from the survivors using a MasterPure Yeast DNA Isolation kit. The DNA was digested overnight at 37 °C with AlwN1 and run on a 0.7% agarose gel. The DNA was transferred to Hybond membranes (GE Life Sciences) by capillary action and blotted using the 400-bp *CIN8* PCR product as a probe. The *CIN8* PCR probe hybridizes to both sides of the AlwNI cut site in *CIN8* (see Fig. 3a), generating bands of 3.2 kb and 6.9 kb in the original strain (PRE; Fig. 4d–f). In most of the FOA^R Can^R strains (Fig. 3), the centromere-proximal 3.2-kb band is retained, indicating that any sequence loss does not extend to this region. Retention of the 6.9-kb band in FOA^R Can^R strains indicates that *CAN1* function has been lost in the absence of an overt DNA rearrangement. In contrast, bands of <6.9 kb are indicative of a GCR event, with fuzzy bands showing sites of telomere addition. In theory, the two bands in Fig. 4d that are between the 6.9 and 3.2 kb bands (in the fifth and seventh lanes from the left) could be either telomere additions of rearrangements. However, based on sequencing results and multiplex PCR, such bands are not likely to be telomere additions.

Chromatin immunoprecipitation. Chromatin immunoprecipitation (ChIP) of asynchronous yeast cells growing in rich medium was performed as described[6,20] and analysed using an iCycleriQ Real-Time PCR detection system (Bio-Rad Laboratories). Rrm3 was C-terminally tagged with 13 Myc epitopes[39]. An anti-Myc monoclonal antibody (Clontech 631206) was used as the anti-serum in ChIP. The amount of DNA in the immunoprecipitate was normalized to the amount in input samples. The ChIP experiment was analysed by qPCR in duplicate or triplicate to obtain an average value for each sample. The ChIP experiment was repeated ≥3 times at each locus. For each qPCR experiment, the amount of signal in the Rrm3 immunoprecipitate was normalized to input and to the immunoprecipitated signal from *ARO1*, a sequence that contains no candidate G4 DNA motif and that has low Rrm3 association[20].

Multiplex PCR. In brief, genomic DNA isolated from *S. cerevisiae* strains before and after GCR events was analysed by multiplex PCR using the primer pairs in Supplementary Table 7 and the following cycling parameters: initial denaturation for 5 min at 95 °C, 35 cycles of 95 °C for 30 s, 56 °C for 30 s, and 72 °C for 45 s, and a final extension at 72 °C for 10 min. PCR products (10 µl per reaction) were run at 90 V on 2.5% agarose gels containing ethidium bromide and visualized by ultraviolet transillumination (for primer sequences, see Supplementary Table 7).

qPCR. The indicated strains were grown in FOA+Can liquid media for 12 h and then transferred to YEPD for 12 h until reaching a concentration of $D_{600\,nm} = 0.5$, and total RNA was isolated using a Quick-RNA MiniPrep kit, including the DNase I treatment, as described by the manufacturer (Zymo Research). cDNA was synthesized from 200 ng DNase I-treated RNA using an iScript One-Step RT–PCR kit with SYBR Green (Bio-Rad) and analysed qPCR using a Bio-Rad CFX96 real-time system. The following primers were used: *URA3* cDNA, 5′-GTTCGACTGATGAGCTATTGAAACT-3′ and 5′-CGACAGTACCCTCATA ACTGAAATC-3′; *CAN1* cDNA 5′-AATATACATCGGGCGTTTAC-3′ and 5′-TCAGCAAGCATCAATAATCC-3′; *ACT1* cDNA, 5′-GTAACATCGTTATGT CCGGTGGTAC-3′ and 5′-CCAAGATAGAACCACCAATCCAGAC-3′. The cycling parameters were: 50 °C for 10 min, 95 °C for 5 min, and 40 cycles of 95 °C for 10 s followed by 57 °C (*ACT1*), 50 °C (*CAN1*), or 55 °C (*URA3*) for 30 s. The data were analysed by the $2^{-\Delta\Delta Ct}$ method[45].

39. Azvolinsky, A., Dunaway, S., Torres, J., Bessler, J. & Zakian, V. A. The *S. cerevisiae* Rrm3p DNA helicase moves with the replication fork and affects replication of all yeast chromosomes. *Genes Dev.* **20,** 3104–3116 (2006).
40. Gueldener, U., Heinisch, J., Koehler, G. J., Voss, D. & Hegemann, J. H. A second set of *loxP* marker cassettes for Cre-mediated multiple gene knockouts in budding yeast. *Nucleic Acids Res.* **30,** e23 (2002).
41. Longtine, M. S. *et al.* Additional modules for versatile and economical PCR-based gene deletion and modification in *Saccharomyces cerevisiae*. *Yeast* **14,** 953–961 (1998).
42. Studier, F. W. Protein production by auto-induction in high density shaking cultures. *Protein Expr. Purif.* **41,** 207–234 (2005).
43. Kushnirov, V. V. Rapid and reliable protein extraction from yeast. *Yeast* **16,** 857–860 (2000).
44. Runge, K. W. & Zakian, V. A. Introduction of extra telomeric DNA sequences into *Saccharomyces cerevisiae* results in telomere elongation. *Mol. Cell. Biol.* **9,** 1488–1497 (1989).
45. Livak, K. J. & Schmittgen, T. D. Analysis of relative gene expression data using real-time quantitative PCR and the $2^{-\Delta\Delta C}{}_T$ method. *Methods* **25,** 402–408 (2001).